Non-coding RNA Research 6 (2021) 15–22

Contents lists available at ScienceDirect

Non-coding RNA Research

journal homepage: www.sciencedirect.com/journal/non-coding-rna-research

Differences of time-dependent microRNA expressions in breast cancer cells

Serife Buket Bozkurt [a,b,*], Bahadir Ozturk [a], Nadir Kocak [c], Ali Unlu [a]

[a] University of Selcuk, Faculty of Medicine, Department of Medical Biochemistry, Konya, Turkey
[b] Hacettepe University, Research Center of Dental Faculty, Ankara, Turkey
[c] University of Selcuk, Faculty of Medicine, Department of Genetic, Konya, Turkey

ARTICLE INFO

Keywords:
miRNA
Discontinuous transcription
MCF-7
MDA-MB-435

ABSTRACT

MicroRNA (miRNA) expression is a dynamic process in the cell, and the proper time period for post-transcriptional regulation might be critical due to the gene-on/-off expression times of the cell. Here, we investigated the effect of different time-points on proliferation, invasion and miRNA expression profiles of human breast cancer cell lines MCF-7 (non-metastatic, epithelium-like breast cancer cell line with oestrogen receptor (ER) positive (+) and human breast cancer cell lines MDA-MB-435 (metastatic, invasive, ER negative (-). For this purpose, MCF-7 and MDA-MB-435 cells were seeded different number in E-plate 16 for proliferation experiment using an electrical impedance-based real-time cell analyzer system (RTCA) for 168 h. Similarly, invasion potential of MCF-7 and MDA-MB-435 were determined by RTCA for 90 h. Total RNAs including miRNAs were isolated at 2, 4, 6, 12, 24, 48 h from the MCF-7 and MDA-MB-435 cells. Afterward, the quantitative 84 miRNA expressions of MCF-7 and MDA-MB-435 were analyzed by Fluidigm Microfluidic 96.96 Dynamic Array. The results of these study demonstrated that both proliferation potential and invasion capacity of MDA-MB-435 is higher than MCF-7 as time-dependent manner. Furthermore, we detected that up/down expressions of 32 miRNAs at all time points in MDA-MB-435 compared to MCF-7 (at least ten-fold increased). Because of the high number of miRNAs, we more closely evaluated the expression of six of them (miR-100–5p, miR-29a-3p, miR-130a-3p, miR-10a-5p, miR-10b-5p, miR-203a), and determined that their levels were dramatically changed by at least 50-fold at different time points of the experiment ($p < 0.01$). The expression levels of five of these miRNAs (miR-100–5p, miR-10a-5p, miR-10b-5p, miR-130a-3p, and miR-29a-3p) started to increase from the fourth hour and continued to increase until the 48th hour in MDA-MB-435 cells compared to MCF-7 cells ($p < 0.01$). Simultaneously, the expression of one of these miRNAs (miR-203a) decreased from the sixth hour to the 48th hour in MDA-MB-435 as compared to MCF-7. We determined pathways associated with target genes using mirPath - DIANA TOOLS. Small RNAs including miRNA are essential regulatory molecules for gene expressions. In the literature, gene expressions have been published as burst and pulse in the form of discontinuous transcription. The data of the research suggested that time-dependent changes of miRNA expressions can be affected target gene transcriptional fluctuations in breast cancer cell and can be base for the further studies.

1. Introduction

Breast cancer is the most common causes of cancer death among women all over the world [1]. This pathology consists of several different subtypes with several morphological appearances, molecular features, biological behaviors, and clinical outcome [2]. This pathology occurs in certain breast tissues, which is then lobular carcinoma or just in the inner lining of the milk ducts [3].

In recent years, a class of tiny non-coding endogenous RNAs, termed miRNAs, was discovered [4]. These post-transcriptional inhibitors may regulate cellular gene expression at target mRNAs through sequence specificity, directing cleavage of the mRNA or translational inhibition [5]. These small molecules are involved in a majority of biological processes such as proliferation, differentiation, apoptosis and pathological processes including invasion, metastasis, epithelial to mesenchymal transition [6]. Further studies have shown that there is a connection between miRNA function and several human malignancies, including breast cancer [7]. More specifically, miRNAs are located in

* Corresponding author. Teaching Assistant Researcher ID: M-5852-2017University of Hacettepe, Faculty of Dentistry, Research Center of Dental Faculty, Ankara, Turkey.
E-mail address: buketbozkurt@hacettepe.edu.tr (S.B. Bozkurt).

https://doi.org/10.1016/j.ncrna.2020.12.001
Received 30 July 2020; Received in revised form 13 December 2020; Accepted 14 December 2020
Available online 19 December 2020

cancer-associated fragile region and suggesting that can regulate pathways containing oncogenic and tumor suppressor genes [8,9]. Additionally, researches have also displayed the association with expression of miRNAs and tumor size, ER positive/negative, metastasis stage [10]. Especially, metastasis feature of mammary tumor cells to invade and migrate to neighboring tissues is important reason for breast cancer mortality [11]. Thus, in this study, human breast cancer cell lines MCF-7 (non-metastatic, epithelium-like breast cancer cell line with ER positive) and human breast cancer cell lines MDA-MB-435 (metastatic, invasive, ER negative) were chosen as the two representative cell lines. As known, gene expression is regulated genetic variants and environmental factors. Additionally, transcriptional fluctuation has been discovered in the cells of diverse species and causes and modulates of discontinuous transcription have been examined in literature. However, the effect of time on gene expression is unknown. Therefore, in the present study, we investigated the effect of different time points on proliferation, invasion, miRNA expressions of MCF-7 and MDA-MB-435 cells.

2. Materials and methods

2.1. Cell culture

MCF-7 and MDA-MB-435 were grown at 37 °C in a humidified, 5% CO_2, 95% air incubator. The culture medium for MDA-MB-435 is Dulbecco's Modified Eagle medium: nutrient mixture F-12 (DMEM/F12) with 2.5 mM L-Glutamine and 15 mM HEPES (Gibco,USA), supplemented with 10% FBS and 1% penicillin-streptomycin. Similarly, MCF-7 cells were grown in DMEM with 1 g/l D-Glucose, 4 mM L-Glutamine, and 1 mM Pyruvate (Gibco,USA), supplemented with 10% FBS and 1% penicillin-streptomycin. The study was approved by Ethics Committee of Medicine Faculty of Selcuk University (2013/198).

2.2. Proliferation of the breast cancer cells

A real-time cell analyzer (RTCA; xCELLigence, ACEA Biosciences, Inc, CA, USA) was used to evaluate the proliferation of human breast cancer cells. Both MDA-MB-435 and MCF-7 of proliferation capacities were investigated by a real-time cell analyzer. Cell index (CI) impedance measurements were performed according to the instructions of the supplier. Both of them were re-suspended in media and subsequently adjusted to 10.000 and 20.000 cells/well. After seeding 100 μl of the cell suspensions into the wells (8 well per each group) of the E-plate 16, human breast cancer cells were monitored every 15 min for a period of 168 h by the RTCA system. MDA-MB-435s and MCF-7s on the E-plate 16, which has 16 wells, were treated every other day with DMEM and DMEM F-12 containing 10% FBS. The values of the electrode impedance were re-presented as the 'cell index'. Cell proliferation experiments were repeated three times.

2.3. Cell invasion evaluation using cell invasion/migration (CIM)-plate

The dynamic cell invasion capabilities of MDA-MB-435s and MCF-7s were deter-mined by RTCA (xCELLigence, ACEA Biosciences, San Diego, CA) using an electronic readout called impedance to quantify adherent cell invasion in real-time. The electrical impedance was displayed as a dimensionless parameter termed cell index (CI). The CI represents the capacity for cell invasion, and the slope of the curve can be related to the invasion velocity of tumor cells. The xCELLigence CI impedance measurements were performed according to the supplier's instructions. The rate of cell invasion was monitored in real-time using modified xCELLigence system cell invasion/migration (CIM)-plates (n = 6). The CIM-plate chambers were designed as gold electrode arrays. In order to perform the experiments, MCF-7 and MDA-MB-435 cells were first deprived of serum for 24 h. Next, the upper section of the chamber was covered in 20 μl of matrigel (Corning Incorporated) diluted in serum-free medium at a ratio of 1:20. Then, the covered section of the chambers was stored at 37 °C in a cell incubator. According to the manufacturer's instructions, 160 μl of 10% FBS DMEM was added to the lower section of the chamber, and 30 μl of se-rum-free DMEM was transferred to the upper section of chamber. These combined chambers were joined in the RTCA Dual Purpose (DP) device at 37 °C with 5% CO_2 for 60 min. The control group was composed of uncoated wells (matrigel-free only migration). To initiate an experiment, 2×10^4 breast cancer cells in 100 μl were added to the upper section of the chamber. The impedance dynamic of each well was measured by the xCELLigence system every 15 min for 90 h, and the results were expressed as a CI value.

2.4. Cell invasion evaluation with transwell-plate

Simultaneously, the cell invasion results were measured using a conventional invasion method (HTS Transwell Invasion). MDA-MB-435 and MCF-7 cells were starved for a 24-h period, then were plated at a density of 2×10^4 cells/well (including 50 μl of serum-free DMEM) in the upper chamber of a matrigel-coated (ratio from 1:10 to 1:20) transwell filter (8.0 μm pore) from Corning. To the reservoir, 150 μl of 10% FBS DMEM and 100 μl of serum-free DMEM were added to the lower and upper chambers. At 24 h, non-invaded cells on the upper side of the matrigel were removed carefully with a cotton swab. The cells bound to the lower side of the filter were washed twice with PBS and fixed with 3.7% formaldehyde at room temperature for 10 min. Fixed cells were washed twice with PBS and stained using 0.1% crystal violet. Invading cells were counted in six random fields, and images were obtained using light microscopy and a camera.

2.5. RNA isolation, complementary DNA (cDNA) synthesis and pre-amplification

Total RNAs (including miRNAs) were isolated from MCF-7 and MDA-MB-435 cell lines by using a High Pure miRNA Isolation Kit (Roche) according to the manufacturer's protocol at 2nd, 4th, 6th, 12th, 24th, 48th hour in the experiment. Purity and integrity of the isolated total RNAs were assessed on the Agilent 2100 bioanalyzer (Agilent Technologies,USA). Then, total RNA samples (2 μl) were converted to cDNA by using miScript II RT Kit cDNA synthesis kits (Qiagen) for miRNA detection. Briefly, 2 μL of total RNAs were added to 5 μl of the reverse transcrition reaction mix (10X miScript Nucleics Mix, 5X miScript HiSpec Buffer, miScript Reverse Transcriptase Mix, DNase, RNase free water) in a total reaction volume of 7 μl. Reverse transcription was performed using the Piko Thermal Cycler (ThermoScientific, USA). cDNA synthesis reaction conditions were: 37 °C for 1 min, 95 °C for 5 min, hold at 4 °C, for 40 cycles). cDNA samples were kept at −80 °C until real-time PCR analysis. We performed a pre-amplification after the reverse transcription using the TaqMan PreAmp Master Mix (Applied Biosystems, Foster City, CA, USA) as well as the Human Primer Pools Set (Exigon, USA). For pre-amplification 2 μl cDNA samples was transferred into a clean 96 pico plate and 8 μl preamplification suspension buffer (5X miScript PreAmp Buffer, HotStartTaq DNA Polymerase, Primer Tool, PreAMP Universal Primer) was added on the top of cDNAs and mixed by pipetting up and down 3–4 times. The pre-amplification cycling conditions were as follows: 95 °C for 10 min, 94 °C for 30 s, 60 °C for 3 min (12 cycles). Then, 1 μl ofexonuclease solution (exonuclease solution and DNA suspension buffer) was added preamplified cDNA samples for eliminate primer dimer. The exonuclease cycling conditions were: 37 °C for 15 min, 95 °C for 5 min.

2.6. High-throughput multiplexed polymerase chain reaction (HTM-PCR)

High-throughput multiplexed polymerase chain reaction (HTM-PCR) experiments were-performed via the BioMark 96.96 dynamic array chip using the high-throughput Bio-Mark real-time PCR system (Fluidigm, South San Francisco, CA). The BioMark 96.96 Dynamic Array is easy to

use because the microfluidic architecture does the work of combining samples and primer-probe sets into 9216 PCR reactions. miRNA PCR Array Human Breast Cancer primers (84 primers) were obtained from miScript Primer Assay (Product No: 331221, Cat. No: MIHS-109ZM-2 Qiagen, France).

Small nucleolar RNA, C/D box 68 (SNORD68); small nucleolar RNA, C/D box 72 (SNORD72); small nucleolar RNA, C/D box 95 (SNORD95); small nucleolar RNA, C/D box 96 A (SNORD96A); small nucleolar RNA, C/D box 61 (SNORD61); and RNA, U6 small nuclear 2 (RNU6-2) were added as potential candidate housekeeping genes in the experiment. At the end of the RT-PCR study, the gene that demonstrated the most stable Ct value, in this case, SNORD61, was used as the internal control. All samples were normalized to this internal control, and fold regulations were calculated using relative quantification (RQ = 2-ΔΔCT). For the h-PCR reaction, pre-amplified cDNA samples were first diluted 1:5 with DNA suspension buffer (Teknova, Hollister, CA, USA). Approximately 360 μL of TaqMan Universal PCR Master Mix (Applied Biosystems, Foster City, CA, USA), 36 μL of 20x GE Sample Loading Reagent (Eva Green, Fluidigm, South San Francisco, CA), 84 μl of DNase, and RNase-free water were mixed, and 3.85 μl of this mixture was pipetted into each well of a 96-well plate. Next, 3.15 μl of a 1:10 dilution of pre-amplified cDNAs were added to the corresponding well in the 96-well plate and mixed. Then, 5 μl of this mixture and 4 μl of 1:1 diluted target primers were pipetted into sub-sequent sample inlets and assay inlets of a 96.96 dynamic array. Next, the BioMark 96.96 dynamic array chip was loaded onto the BioMark integrated fluidic circuit (IFC) controller HX (Fluidigm, San Francisco, USA) to distribute the assay mix and sample mix from the loading inlets into the BioMark 96.96 dynamic array reaction chambers for qRT-PCR by Fluidigm's integrated fluidic circuit technology. The thermal protocol was performed using the Biomark System as follows: 50 °C for 2 min, 70 °C for 30 min, 25 °C for 10 min, and 95 °C for 10 min, followed by 24 cycles of 94 °C for 15 s, 55 °C for 30 s and 70 °C for 30 s. Finally, a melting curve cycle of 60°C–95 °C for 1 min concluded the protocol.

2.7. Statistical analyses

For proliferation and invasion experiments, the statistical analysis was used analysis of variance (ANOVA) and Tukey HSD multiple comparison tests. The data are represented as mean ± standard deviation. A value of $p < 0.05$ was considered to be statistically significant. RT-PCR experiments of statistical analyses were performed using the Biogazelle qbase PLUS 2.0 software. The gene expression data normalization process was performed via the 2-ΔΔCt method, which is based on the relative quantification method (normalized threshold cycle (Ct) value of sample minus normalized Ct value of control). The averages of the technical replicates of the normalized data of the groups were compared with the student's *t*-test. $P < 0.05$ was considered statiscally significant.

3. Results

3.1. Real-time cell proliferation analysis

To evaluate dynamic cellular proliferation of human breast cancer cells (MCF-7, MDA-MB-435) were seeded at different cell counts in 16 E-plates. Then, each group (include 10.000, 20.000 cells/well) was monitored every 15 min for 168 h and cell number, viability, morphology and adherence of cells were determined by sensor electrical impedance. Statistical analysis demonstrated that proliferation curves of MCF-7 and MDA-MB-435 reflected as paralell with cell number in group (Fig. 1). According to the data obtained from the RTCA, 10.000 cell/well of MCF-7 reached to minimum cell number at 15th hour and these groups achived maximum cell number at 130th hour ($p < 0.05$). While 20.000 cell/well group of MCF-7 was minimum cell number at 15th hour and maximum cell number 55th hour ($p < 0.05$). Additionally, 10.000 cell/well of MDA-MB-435 were displayed minimum cell number value at 15th hour and maksimum cell number value at 100th hour ($p < 0.05$). Whereas, 20.000 cell/well group of MDA-MB-435 was assigned minimum cell number at 20th hour and maksimum cell number at 100th hour, ($p < 0.05$). Also, the results from the repeated measurements of the data for 168 h displayed that there was a significant difference between the MCF-7 and MDA-MB-435 cells and that the aggressiveness of the cell proliferation was higher in MDA-MB-435 cells ($p < 0.05$).

3.2. Real-time measurement of cell invasion in breast cancer cells

The cell invasion capacities of the breast cancer cell lines were measured with the xCELLigence platform. MCF-7 and MDA-MB-435 breast cancer cells were added at 20.000 cells per matrigel-coated or uncoated well in CIM-plates (n = 6). Then, the cells were monitored every 15 min for the indicated period of time. The impedance CI of the coated wells for the MDA-MB-435 was seen to increase greatly after

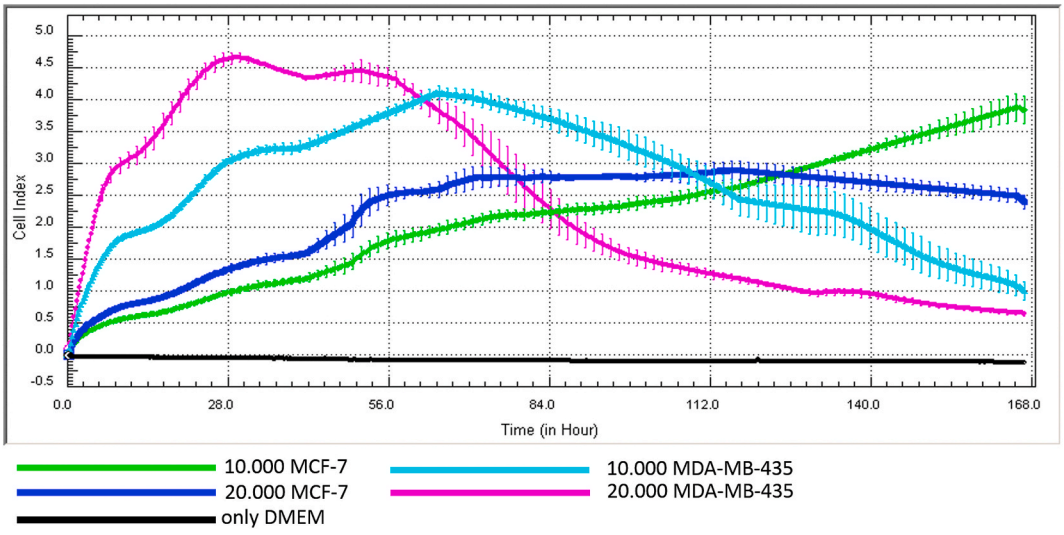

Fig. 1. Real time analysis of proliferation graph of MCF-7 and MDA-MB-435 cells using E-plate 16. Notes: The MCF-7 and MDA-MB-435 cells seeded to 10.000 and 20.000 cell per well into the E-plate-16 (n = 8), respectively. As shown in the graphs, the aggressiveness of different cell number of MDA-MB-435 (10.000 cell per well- turquoise curve; 20.000 cell per well-pink curve) was higher than different cell number of MCF-7 (10.000 cell per well-green curve; 20.000 cell per well-blue curve) ($p < 0.05$).

seeding, up to its maximum value, from 5 to 25 h. Additionally, this situation determined at 5 h and reached its second maximum at 28 h in MCF-7 (Fig. 2). The invasion capacity of the MDA-MB-435 cells was significantly higher than the invasion capacity of MCF-7 ($p < 0.05$).

3.3. Matrigel invasion capacities of breast cancer cells

The invasion potential of MDA-MB-435 and MCF-7 cells was next examined using a matrigel invasion assay. As a result of this experiment, it was determined that the number of invasive cells in both the 1:10 and 1:20 matrigel MCF-7 samples were significantly lower than those of the matrigel-free control group ($p < 0.001$; Fig. 3). The invasive cell assay results obtained from the MDA-MB-435 cells showed a significantly lower ($p < 0.001$) number of invasive cells in the 1:10 matrigel-coated group than the control group. Furthermore, it was determined that the number of invasive cells in the 1:20 matrigel-coated group of the same cell line was statistically more invasive than that of the control group ($p < 0.05$; Fig. 3). Thus, MDA-MB-435 cells are dramatically more invasive than MCF-7 cells.

3.4. The effects of time-points on miRNA expressions of breast cancer cells

The expression of 84 breast cancer-related miRNAs were analyzed in MDA-MB-435 versus MCF-7 at six different time periods ranging from 2 to 48 h using Fluidigm Microfluidic 96.96 Dynamic Array. MDA-MB-435 time-dependent groups (2nd hour, 4th hour, 6th hour, 12th hour, 24th hour, 48th hour) were compared to MCF-7 time-dependent groups (2nd hour, 4th hour, 6th hour, 12th hour, 24th hour, 48th hour) and we evaluated the fold regulations above 10 and consistently up or down-regulated ($p < 0.001$). Statistical analysis demonstrated that 32 miRNAs included both up- and down-regulated expressions of miRNAs were differentially expressed by at least ten-fold. Then, we determined that 11 miRNAs of 32 miRNAs were differentially expressed at the 2nd hour. Continuing from hour two, 23 miRNAs were differentially expressed at the 4th hour, 16 miRNAs at the 6th hour, 13 miRNAs at the 12th hour, 13 miRNAs at the 24th hour, and 15 miRNAs at the 48th hour in MDA-MB-435 versus MCF-7 (over ten-fold up-/down-regulated) (Table 1). Following this analysis, we further evaluated the miRNAs that demonstrated differences of greater than 50x in expression levels. According to these data, the first time point (2nd hour) had three miRNAs including miR-100–5p, miR-10b-5p, miR-130a-3p that were over 50-fold up regulated and there was also one miRNA (miR-203a) that was down-regulated by over 50-fold ($p < 0.001$). Additionally, eight miRNAs (miR-100–5p, miR-10a-5p, miR-10b-5p, miR-222–3p, miR-130a-3p, miR-29a-3p, miR-29c-3p, miR-125b-5p) were displayed increasing 50X fold-regulation at the 4th hour ($p < 0.001$). Subsequently, we determined four miRNAs (miR-10a-5p, miR-100–5p, miR-10b-5p, miR-130a-3p) at 6th hour and three miRNAs (miR-10a-5p, miR-100–5p, miR-130a-3p) at 12th hour ($p < 0.001$). Also, four miRNAs (miR-10a-5p, miR-10b-5p, miR-100–5p, miR-130a-3p) at 24th hour, and six miRNAs (miR-100–5p, miR-10a-5p, miR-125b-1-3p, miR-130a-3p, miR-222–3p, miR-204–5p) at 48th hour were determined that all had a greater than 50-fold change in MDA-MB-435 cells when compared to the MCF-7 ($p < 0.001$) (Table 1). Especially, six miRNAs that were observed to be dramatically differentially expressed in MDA-MB-435s when compared to MCF-7s (Fig. 4). There was large difference for miR-100–5p, miR-10a-5p, and miR-10b-5p, which showed a 200–1000 fold difference between the 2nd and 48th hours of the experiment ($p < 0.01$). miR-100–5p, which is defined as both an oncomir and a tumor suppressor, displayed an increase in expression that began from the 2nd hour and continued to the 48th hour of the experiment. The highest fold change was determined for this miRNA at the 4th hour, with an up-regulation of 1,032x. Furthermore, miR-10a-5p and miR-10b-5p, which are members of the miR-10 family, were observed to be significantly up-regulated at the 4th hour by 912-fold. Additionally, miR-130a-3p and miR-29a-3p were up-regulated 10–181x in MDA-MB-435 cells when compared to MCF-7. On the other hand, miR-203a displayed a consistent down-regulation across all of the time periods measured. The results of our continuously expressed miRNAs and their functions were consistent with the literature.

3.5. Possible pathway analysis of the dysregulated miRNAs

To evaluate the potential role of the choosed 11 miRNAs in malign breast cancer, possible targets assessment were conducted using the DIANA TOOLS (di-ana.imis.athena-innovation.gr) platform. Many genes were predicted as targets of the selected miRNAs. We next utilized mirPath from DIANA TOOLS to analyze the feasible pathways that contained putative target genes of the selected miRNAs. Our study demonstrated that the set of genes regulated by the six dysfunctional miRNAs have key roles in various pathways, such as the mTOR signaling

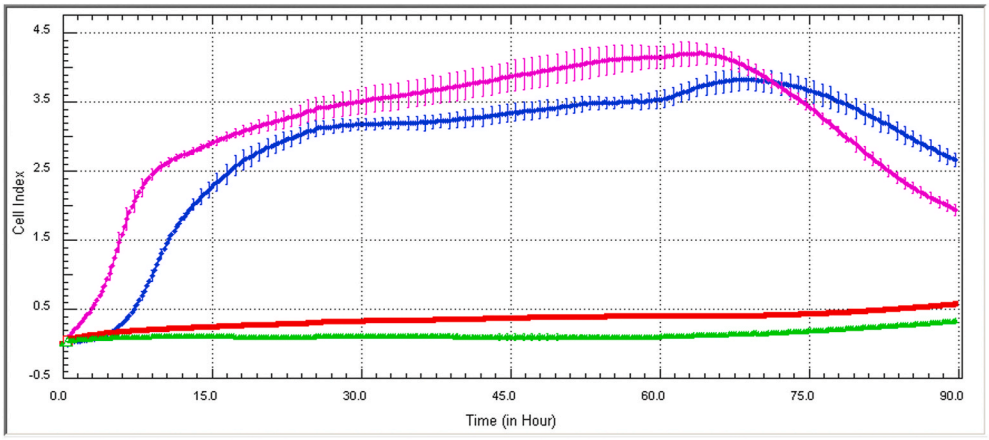

Fig. 2. Comparison of MCF-7 and MDA-MB-435 cell invasion capacities generated by real-time cell analyzer measuring impedance-based signals. MCF-7 (20.000 cell per well; green curve) and MDA-MB-435 (20.000 cell per well; green curve) were seeded in a 1:20 (v/v) Matrigel-coated CIM-Plate 16 with 10% serum serving as the chemoattractant in the lower chamber. The rate of invasion was monitored in real-time using the RTCA system. Comparison of cell index between the MCF-7 cells (green curve) and MDA-MB-435 cells (blue curve) invading the matrigel layer towards 10% FBS DMEM, during 90 h ($p < 0.05$, $n = 6$).

	Upper Chamber	Lower Chamber
	SF+MDA-MB-435	% 10 FBS (Control)
	SF+MDA-MB-435	Matrigel (1:20)-% 10 FBS
	SF+MCF-7	% 10 FBS (Control)
	SF+MCF-7	Matrigel (1:20)-% 10 FBS

SF: Serum Free
FBS:Foetal Bovine Serum

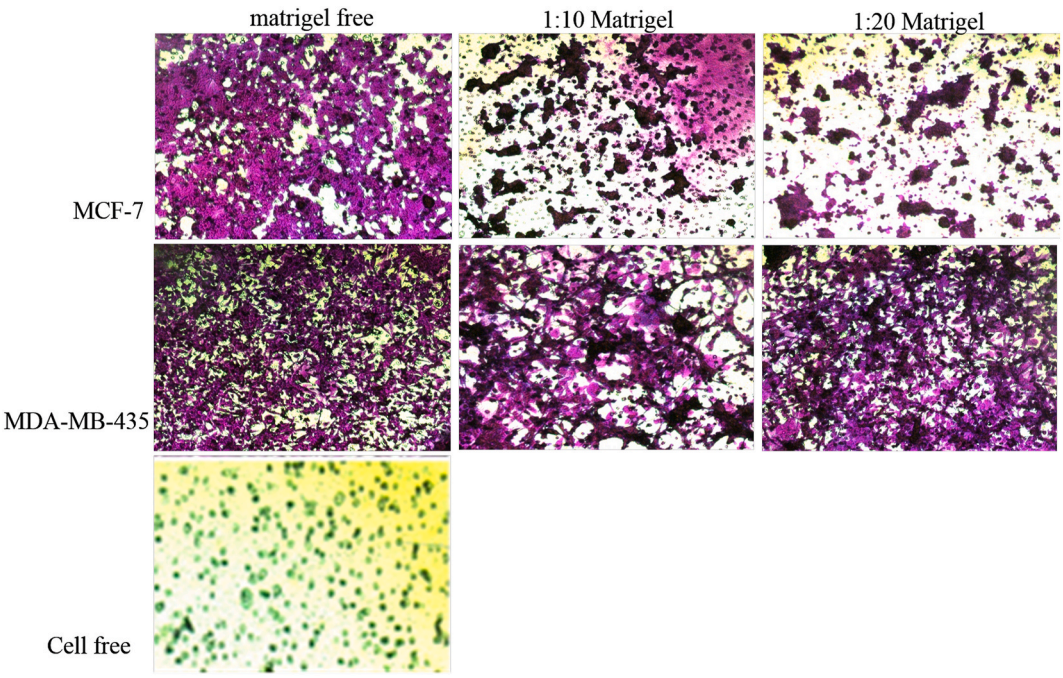

Fig. 3. Photographs of polycarbonate filters coated with Matrigel from transwell-plate chemoinvasion assays. Invaded MCF-7 cells in 1:10 matrigel, 1:20 matrigel and invaded MDA-MB-435 cells in 1:10 matrigel, 1:20 matrigel.

pathway (hsa 04150), ErbB signaling pathway (hsa 04012), PI3K-Akt signaling pathway (hsa 04151), Wnt signaling pathway (hsa 04310), and p53 signaling pathway (hsa 04115) (Fig. 5).

4. Discussion

MicroRNAs are small endogenous RNAs that perform as post-transcriptional regulators of gene expression in cellular functions including proliferation, differentiation and cell growth in animals, viruses, plants [12]. There is accumulating evidence that miRNA expression profiles differ between breast cancer and healthy breast tissue [6,13,14]. Recent advanced studies have monitored transcriptional pulsing in eukaryotes at multiple time points [15], and the gene-on and gene-off times have been shown to be highly important for post-transcriptional regulation. In this current study, we examined that the effect of different time-points on proliferation, invasion and miRNA expression profiles of human breast cancer cell lines MCF-7 (non-metastatic, epithelium-like breast cancer cell line with ER positive) and human breast cancer cell lines MDA-MB-435 (metastatic, invasive, ER negative). The results displayed that proliferation potential and invasion capacity of MDA-MB-435 cells higher than MCF-7 cells. Additionally, we determined that total RNA including miRNAs isolation at different time-points affected 32 miRNA expressions (onco-miRs, tumor suppressor-miRs) as up/down in MDA-MB-435 cells compared to MCF-7 ($p < 0.01$). Especially, miR-100–5p, miR-29a-3p, miR-130a-3p, miR-10a-5p, miR-10b-5p and miR-203a significantly displayed different expression in MDA-MB-435 cells compared to MCF-7 at all time periods ($p < 0.01$). Functional studies reported that miR-100 have the ability to target numerous biomolecules that are important in carcinogenesis, which makes it possible to function as both a tumor promoter and tumor suppressor [16]. Evidence is accumulating that dysregulation and aberrant expression of miR-100 is strongly implicated in the development of diagnostic and/or prognostic marker for breast cancer [16]. In our study determined that miR 100–5p continuously displayed high expression in MDA-MB-435 cells compared to MCF-7 cells at all time points and it seems to be an important part of invasive characteristic of the cell. Luo et al. determined that miR-100 expression of more invasive breast cancer cell lines higher than less invasive breast cancer cell lines and non-tumorigenic breast epithelial cell lines [17]. Similar to the results of Zhong et al. detected that five up-regulated miRNAs such as miR-100, miR-29a, miR-196a, miR-222, miR-30a in two resistant sublines of MCF-7 compared to MCF-7/S [18]. miR-29a-3p is largely described as an oncomir in literature [14,19,20] and it displayed high expression in most of the cancer. In the present study, miR-29a-3p expression was determined different time periods (4th,6th, 24th,48th) and the highest expression of miR-29a-3p was detected at 4th hour. Wu et al. demonstrated that miR-29–3p levels significantly increased in the serum of breast cancer patients compared to the healthy control and they suggested that miR-29a-3p can an usefull biomarker for breast cancer [21]. Notably, target genes of miR-29a-3p regulate function of some transcription factors including methyltransferase, cell cycle control, cell differentiation, apoptosis and metastasis [22,23][22,23] and it increase metastatic behavior of cancer by induce EMT [24]. In addition, our results revealed that high miR-29a-3p expression in more invasive breast cancer cell and our findings are consistent with findings of literature. miR-130a-3p and miR-130b-3p are described as a member of 130 family and miR-130a-3p promote vascular endothelial cell proliferation and angiogenesis in tumor [25]. In literature, there little is study the effect of miR-130 family on cancer associated genes both oncogene and tumor suppressor. Zong et al. demonstrated that miR-130b-3p induce proliferation, differentiation and angiogenesis in ovarian cancer cell lines and their results were also described as a marker for the drug resistance of ovarian carcinoma [26]. Also, literature reported that the effect of miR-130b in breast cancer are due to chemoresistance and proliferation suppression via the PI3K/Akt pathway [27]. In the present study, we examined miR-130a-3p and miR-130b-3p expressions at different time points and miR-130a-3p expression was determined higher than miR-130b-3p as continuously.

Transcriptional pulsing has been observed in both prokaryotes and eukaryotes and plays a important role in cell-to-cell diversity of protein and mRNA numbers. Also, time constants associated with episodes of transcriptional bursting and mRNA degradation lead to different cellular mRNA distributions [28]. Transcription of genes can be discontinuous, happening in pulses or bursts. Especially, gene displayed its own transcriptional signature, differing in probability of firing and pulse duration [29]. However, some miRNAs were continuously overexpressed during

Table. 1
Differential expression of miRNAs in invasive and less invasive breast cancer cells.

	MicroRNA	Time-points											
		2nd hour		4th hour		6th hour		12th hour		24th hour		48th hour	
		Fold-regulation	P value	Fold-regulation	P value	Fold-regulation	P value	Fold-regulation	P value	Fold-regulation	P value	Fold-regulation	P value
1	miR-100–5p	632	0.000001	1032	0.003596	515	0.000253	315	0.000012	87	0.000249	656	0.000008
2	miR-10a-5p			912	0.002802	533	0.000176	350	0.000002	398	0.000574	521	0.000052
3	miR-10b-5p	241	0.00034	536	0.002267	209	0.000169			218	0.000289		
4	miR-130a-3p	92	0.000778	181	0.000036	103	0.000001	87	0.000249	105	0.000112	126	0.000415
5	miR-130b-3p	15	0.001112	30	0.000088	17	0.000011	23	0.000003	18	0.000455	13	0.000387
6	miR-125b-5p			50	0.000248					35	0.000233	484	0.011749
7	miR-181a-5p	12	0.002337					10	0.000071				
8	miR-181c-5p	10	0.002049			12	0.000018						
9	miR-203a	−331	0.000079	−14	0.000913	−48	0.00002			−36	0.000588	−19	0.000776
10	miR-489–3p	−15	0.000023										
11	miR-200b-3p							−5	0.000001				
12	miR-200c-3p	−11	0.00042			−8	0.000001	−7	0.000003				
13	miR-222–3p			223	0.000765							124	0.000001
14	miR-29a-3p			65	0.003471	39	0.000002			38	0.000002	42	0.000052
15	miR-29b-3p			29	0.012499			15	0.001189			16	0.000762
16	miR-29c-3p			53	0.001857	31	0.000065	28	0.000004			38	0.000443
17	miR-125b-5p					33	0.000204					34	0.001059
18	miR-18a-5p	10	0.000001	45	0.0092	14	0.00504			12	0.01023		
19	miR-19a-3p			43	0.034015	10	0.003065	12	0.000002	11	0.02361		
20	miR-19b-3p			35	0.029604			11	0.000005	10	0.016404		
21	miR-20a-5p			18	0.006415								
22	miR-20b-5p			17	0.002549								
23	miR-17–5p			15	0.002111								
24	miR-140–5p			13	0.030292								
25	miR-22–3p			10	0.001717								
26	miR-424–5p											10	0.000037
27	miR-1			18	0.005689								
28	miR-205–5p			−7	0.000225	−15	0.000011			−16	0.000023	−18	0.000081
29	miR-181b-5p					12	0.000018						
30	miR-141–3p					−11	0.000004	−9	0.000239	−15	0.000043	−10	0.000001
31	miR-204–5p			39	0.028008							117	0.001091
32	miR-424–5p			25	0.010959								

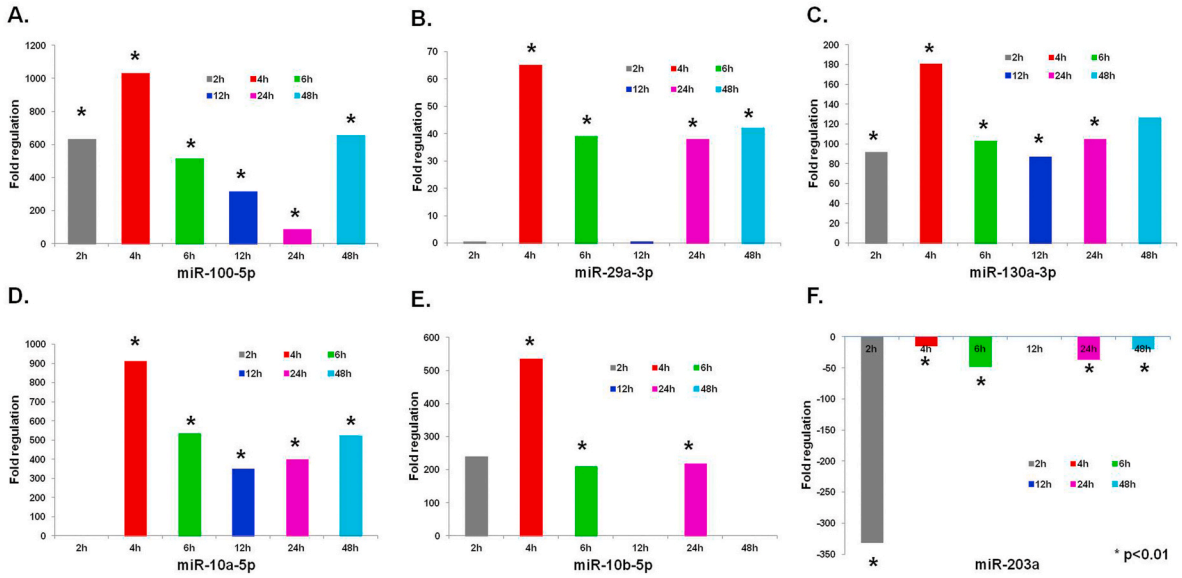

Fig. 4. Dramatically expressed ($p<0.01$) of six miRNAs in MDA-MB-435 cells compared to MCF-7 cells for different time points (2, 4, 6, 12, 24, 48h).

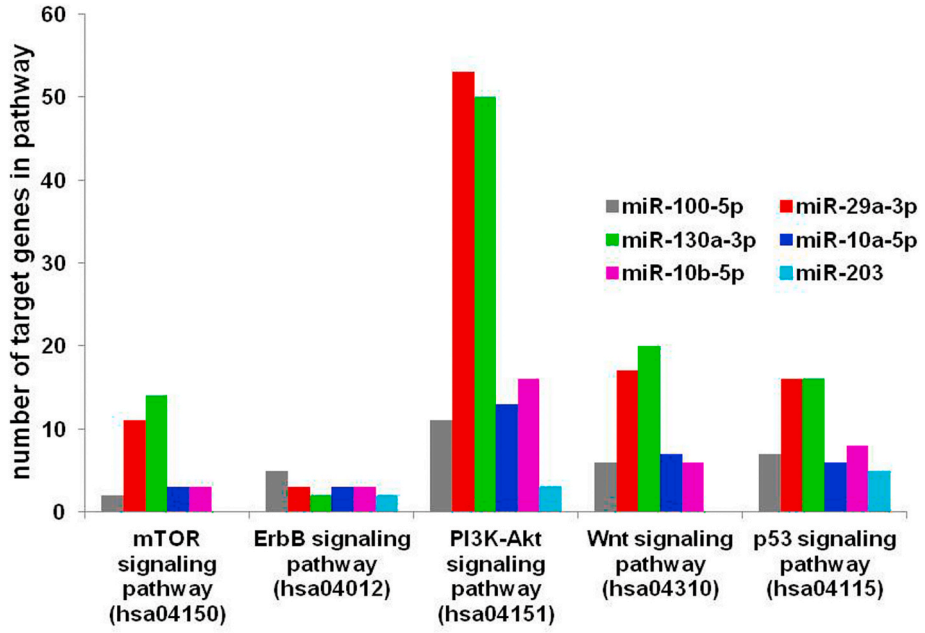

Fig. 5. The numbers of target genes regulated by these 6 dramatically expressed miRNAs ($p<0.05$) in pathways as analyzed by mirPath-DIANA TOOLS.

breast cancer development. We displayed that quantitatively profiled miR-10a-5p and miR-10b-5p changed time dependent in MDA-MB-435 cells compared to MCF-7. Similarly, Ma et al. and Edmonds et al. determined that level of miR-10b-5p in metastatic cells (X50 fold regulation) higher than normal breast epithelial cells [30,31]. In addition, other studies in literature supported that miR-10b-5p expression increased in breast cancer tissues [32] and these studies suggested that miR-10b-5p can be describe as a marker for the metastatic breast cancer [33,34]. Ahmad et al. revealed that miR-10b mediated induction of drug resistance through down-regulation of HDAC4 in tamoxifen resistance of ER-positive breast cancer cells [35]. hsa-miR-203a has been described as an anti-tumorigenic [36] and anti-proliferative action via inhibiting of MAPK pathway in invasive breast cancer cell [37]. More importantly, recent reports indicated that miR-203a has high potential for breast cancer treatment by both increasing drug sensitivity [38] and preventing metastasis [39]. Our results displayed that miR-203a-3p expression decreased at all time points and these results were reflected at the most at 2nd hour. Zhang et al. indicates that miR 203a-3p levels decreased in metastatic breast cancer cell lines compared to primary and non-metastatic breast cancer [40]. Also, Wang et al. suggested that elevated levels of miR 203a-3p levels inhibits cell proliferation and can be a usefull therapeutic target [41].The lack of evaluation of miRNAs and predicted target genes mRNA expression levels were the limitation of this study. Confirmation of miRNAs and predicted target genes mRNA expressions would substantially improve our data in the breast cancer cells.

5. Conclusion

In conclusion, the findings of this study suggest that miRNA expression levels may be change with different time points in breast cancer cells. We believe that the increase and decrease in miRNA

expression levels stem from an expression rhythm in the cells, and this flux might be related to the pathophysiology of breast cancer. Also, time-dependent miRNA expressions can provide new perspectives for both intracellular miRNA expression levels and the miRNA regulation of target genes in physiologic pathways.

Declaration of competing interest

The authors declare they have no conflict of interest.

CRediT authorship contribution statement

Serife Buket Bozkurt: Investigation, Formal analysis, Writing - original draftWriting – original draft, Writing - review & editingWriting – review & editing, Carried out the experiment. **Bahadir Ozturk:** Formal analysis. **Nadir Kocak:** Formal analysis. **Ali Unlu:** Project administration.

Acknowledgments

This study was made possible with financial support from Selcuk University Research Coordination Office, Konya, Turkey, for the project 13202042. This work was performed at Selcuk University, Research Laboratory of Biochemistry Department, Konya, Turkey. We thank Dr. Kahraman Tanrıverdi (Department of Medicine, Division of Cardiovascular Medicine, University of Massachusetts Medical School, Worcester, Massachusetts, USA) for assistance with HTM-PCR analysis of human breast cancer cells.

References

[1] B.D.A. Pultz, F.A.C. Luz, P.R. Faria, A.P.L. Oliveira, R.A. de Araújo, M.J.B. Silva, Far beyond the usual biomarkers in breast cancer: a review, J. Canc. (2014) 559–571.
[2] S. Volinia, M. Galasso, M.E. Sana, Breast cancer signatures for invasiveness and prognosis defined by deep sequencing of microRNA, Proc. Natl. Acad. Sci. Unit. States Am. (2012) 3024–3029.
[3] H.S. Han, A.M. Magliocco, Molecular testing and the pathologist's role in clinical trials of breast cancer, Clin. Breast Canc. (2016) 166–179.
[4] J. Makarova, M.U. Shkurnikov, D. Wicklein, Intracellular and extracellular microRNA: an update on localization and biological role, Prog. Histochem. Cytochem. (2016) 33–49.
[5] D.P. Bartel Dp, MicroRNAs genomics biogenesis, mechanism, and function, Cell (2004) 281–297.
[6] J. Zhu, Z. Zheng, J. Wang, X. Cheng, Different miRNA expression profiles between human breast cancer tumors and serum, Front. Genet. 5 (2014) 149.
[7] K. Ruan, X. Fang, G. Ouyang, MicroRNAs: novel regulators in the hallmarks of human cancer, Canc. Lett. (2009) 116–126.
[8] G. Di Leva, C.M. Croce, Roles of small RNAs in tumor formation, Trends Mol. Med. 16 (6) (2010) 257–267.
[9] L. Zhang, J. Huang, N. Yang, J. Greshock, M.S. Megraw, A. Giannakakis, microRNAs exhibit high frequency genomic alterations in human cancer, Proc. Natl. Acad. Sci. U.S.A. (2006) 9136–9141.
[10] M.V. Iorio, M. Ferracin, C.G. Liu, A. Veronese, R. Spizzo, S. Sabbioni, MicroRNA gene expression deregulation in human breast cancer, Cancer Res. 65 (2005) 7065–7070.
[11] S. Valastyan, R.A. Weinberg, Tumor metastasis: molecular insights and evolving paradigms, Cell 147 (2011) 275–292.
[12] T.X. Lu, M.E. Rothenberg, MicroRNA, J. Allergy. Clin. Immunol (2018) 1202–1207.
[13] D. Luo, J.M. Wilson, N. Harvel, A systematic evaluation of miRNA:mRNA interactions involved in the migration and invasion of breast cancer cells, J. Transl. Med. 11 (2013) 57.
[14] J. Le Quesne, C. Caldas, Micro-RNAs and breast cancer, Mol. Oncol. (2010) 230–241.
[15] J.R. Chubb, T. Trcek, S.M. Shenoy, R.H. Singer, Transcriptional pulsing of a developmental gene, Curr. Biol. (2006) 1018–1025.
[16] C. Qin, R.Y. Huang, Z.X. Wang, Potential role of miR-100 in cancer diagnosis, prognosis, and therapy, Tumor Biol. (2015) 1403–1409.
[17] D. Luo, J. M Wilson, N. Harvel, J. Liu, L. Pei, S. Huang, A systematic evaluation of miRNA:mRNA interactions involved in the migration and invasion of breast cancer cells, J. Transl. Med. 11 (2013) 57.
[18] S. Zhong, W. Li, Z. Chen, J. Xu, J. Zhao, MiR-222 and miR-29a contribute to the drug-resistance of breast cancer cells, Gene (2013) 8–14.
[19] S.A. Melo, M. Esteller, Dysregulation of microRNAs in cancer: playing with fire, FEBS Lett. (2011) 2087–2099.
[20] E. Tormo, B. Pineda, E. Serna, A. Guijarro, G. Ribas, J. Fores, MicroRNA profile in response to doxorubicin treatment in breast cancer, J. Cell. Biochem. (2015) 2061–2073.
[21] Q. Wu, C. Wang, Z. Lu, L. Guo, Q. Ge, Analysis of serum genome-wide microRNAs for breast cancer detection, Clin. Chim. Acta (2012) 1058–1065.
[22] Y. Wang, X. Zhang, H. Li, The role of miRNA-29 family in cancer, Eur. J. Cell Biol. 92 (3) (2013) 123–128.
[23] C.A. Gebeshuber, K. Zatloukal, J. Martinez, miR-29a suppresses tristetraprolin, which is a regulator of epithelial polarity and metastasis, EMBO Rep. (2009) 400–405.
[24] H. Jiang, G. Zhang, J.H. Wu, C.P. Jiang, Diverse roles of miR-29 in cancer, Oncol. Rep. (2014) 1509–1516, review.
[25] K. Boll, K. Reiche, K. Kasack, N. Mörbt, A.K. Kretzschmar, J.M. Tomm, MiR-130a, miR-203 and miR-205 jointly repress key oncogenic pathways and are downregulated in prostate carcinoma, Oncogene (2013) 277–285.
[26] C. Zong, J. Wang, T. Shi, MicroRNA 130b enhances drug resistance in human ovarian cancer cells, Tumour. Biol. (2014) 12151–12156.
[27] Y. Miao, W. Zheng, N. Li, Z. Su, L. Zhao, H. Zhou, L. Jia, MicroRNA-130b targets PTEN to mediate drug resistance and proliferation of breast cancer cells via the PI3K/Akt signaling pathway, Sci. Rep. 6 (7) (2017) 1–12, 41942.
[28] S. Iyer-Biswas, F. Hayot, C. Jayaprakash, Stochasticity of gene products from transcriptional pulsing, Phys. Rev. E - Stat. Nonlinear Soft Matter Phys. 79 (2009).
[29] T. Muramoto, D. Cannon, M. Gierlinski, A. Corrigan, G. J Barton, J.R. Chubb, Live imaging of nascent RNA dynamics reveals distinct types of transcriptional pulse regulation, Proc. Natl. Acad. Sci. U.S.A. (2012) 7350–7355.
[30] L. Ma, J. Teruya-Feldstein, R.A. Weinberg, Tumour invasion and metastasis initiated by microRNA-10b in breast cancer, Nature (2007) 682–688.
[31] M.D. Edmonds, D.R. Hurst, K.S. Vaidya, L.J. Stafford, D. Chen, D.R. Welch, Breast cancer metastasis suppressor 1 coordinately regulates metastasis-associated microRNA expression, Int. J. Canc. (2009) 1778–1785.
[32] W. Min, B. Wang, J. Li, J. Han, Y. Zhao, W. Su, et al., The expression and significance of five types of miRNAs in breast cancer, Med. Sci. Monit. Basic. Res. (2014) 97–104.
[33] Y. Liu, J. Zhao, P.Y. Zhang, MicroRNA-10b targets E-cadherin and modulates, Med. Sci. Mon. Int. Med. J. Exp. Clin. Res. (2012) 299–308.
[34] M. Li, Role of miR-10b in breast cancer metastasis, Breast Canc. Res. 12 (5) (2010) 210.
[35] A. Ahmad, K.R. Ginnebaugh, S. Yin, A. Bollig-Fischer, K.B. Reddy, F.H. Sarkar, Functional role of miR-10b in tamoxifen resistance of ER-positive breast cancer cells through down-regulation of HDAC4, BMC Cancer 24 (2015) 1–10, 15:540.
[36] E. D'Ippolito, M.V. Iorio, MicroRNAs and triple negative breast cancer, Int. J. Mol. Sci. (2013) 22202–22220.
[37] J. Chen, U.M. Tran, U. Rajarajacholan, S. Thalappilly, K. Riabowol, ING1b-inducible microRNA203 inhibits cell proliferation, Br. J. Canc. (2013) 1143–1148.
[38] S. Aakko, A.H. Straume, E.E. Birkeland, P. Chen, X. Qiao, P.E. Lønning, M.J. Kallio, MYC-induced miR-203b-3p and miR-203a-3p control Bcl-xL expression and paclitaxel sensitivity in tumor cells, Transl. Oncol. 12 (1) (2019) 170–179.
[39] J. Xu, C. Shao, X. Wang, X. Zhao, J. Chen, Y. Ouyang, J. Feng, F. Zhang, et al., circTADA2As suppress breast cancer progression and metastasis via targeting miR-203a 3p/SOCS3 axis, Cell Death Dis. 10 (3) (2019) 175.
[40] Z. Zhang, B. Zhang, W. Li, L. Fu, L. Fu, Z. Zhu, et al., Epigenetic Silencing of miR-203 Upregulates SNAI2 and Contributes to the Invasiveness of Malignant Breast Cancer Cells, Genes & cancer, 2011, pp. 782–791.
[41] C. Wang, X. Zheng, C. Shen, Y. Shi, MicroRNA-203 suppresses cell proliferation and migration by targeting BIRC5 and LASP1 in human triple-negative breast cancer cells, J. Exp. Clin. Canc. Res. (2012) 1–8.